

Article

A Green Blue LED-Driven Two-Liquid-Phase One-Pot Procedure for the Synthesis of Estrogen-Related Quinol Prodrugs

Elisa De Marchi , Lorenzo Botta , Bruno Mattia Bizzarri  and Raffaele Saladino * 

Department of Biological and Ecological Sciences, University of Tuscia, 01100 Viterbo, Italy

* Correspondence: saladino@unitus.it

Abstract: Quinol derivatives of estrogens are effective pro-drugs in steroid replacement therapy. Here, we report that these compounds can be synthesized in one-pot conditions and high yield by blue LED-driven photo-oxygenation of parent estrogens. The oxidation was performed in buffer and eco-certified 2-methyltetrahydrofuran as the two-liquid-phase reaction solvent, and in the presence of meso-tetraphenyl porphyrin as the photosensitizer. Two steroidal prodrugs 10 β , 17 β -dihydroxyestra-1,4-dien-3-one (DHED) and 10 β -Hydroxyestra-1,4-diene-3,17-dione (HEDD) were obtained with high yield and selectivity.

Keywords: estrogens; estrogen-related quinols; prodrug; CNS-selective estrogen therapy; DHED; HEDD; neuroprotection; para-quinol; photo-oxygenation; photochemistry



Citation: De Marchi, E.; Botta, L.; Bizzarri, B.M.; Saladino, R. A Green Blue LED-Driven Two-Liquid-Phase One-Pot Procedure for the Synthesis of Estrogen-Related Quinol Prodrugs. *Molecules* **2022**, *27*, 8961. <https://doi.org/10.3390/molecules27248961>

Academic Editor: Cristobal De Los Rios

Received: 16 November 2022

Accepted: 14 December 2022

Published: 16 December 2022

Publisher's Note: MDPI stays neutral with regard to jurisdictional claims in published maps and institutional affiliations.



Copyright: © 2022 by the authors. Licensee MDPI, Basel, Switzerland. This article is an open access article distributed under the terms and conditions of the Creative Commons Attribution (CC BY) license (<https://creativecommons.org/licenses/by/4.0/>).

1. Introduction

Estrogens are steroidal hormones characterized by a variety of biological effects, including anti-cancer activity, prevention of heart diseases, and neuroprotection [1]. In addition, they are applied in Hormone Replacement Therapy (HRT) for the prevention of chronic diseases in post-menopausal women. Unfortunately, current estrogen therapy is limited due to the presence of undesired side effects [2–4], such as increased risk of breast cancer [5], thromboembolism, coronary heart disease, and stroke [6,7]. As a result, analogues of estrogens are required to counteract the side effects. Quinol derivatives of estrogens are effective pro-drugs for this HRT. They are converted to corresponding estrogens in the brain, remaining inactive in the rest of the body. This allows the efficient treatment of neurological and psychiatric diseases, without emergence of peripheral side effects [3,8,9]. In this framework, 10 β , 17 β -dihydroxyestra-1,4-dien-3-one (DHED), received a particular attention as an alternative to 17 β -estradiol. In vitro and in vivo studies showed that DHED has the potential to treat menopausal symptoms [9], ocular neurodegenerations (including glaucoma) [10,11], androgen deprivation-associated hot flushes [12], and Alzheimer's [13] and Parkinson's neurological disorders [14]. Estrogen-related quinols are synthesized by the oxygenation of the phenolic A-ring of the molecule [15–21], the procedure being limited by the use of stoichiometric oxidants (e.g., oxone [22], hypervalent iodine [23,24], and excess of hydrogen peroxide H₂O₂ [25]). As an alternative, dye-sensitized photo-oxygenation of 17 β -estradiol **1a** has been reported to yield mixtures of the corresponding hydro-peroxide **2a** and DHED **3a** [26] (the structures of compounds **1a**, **2a** and **3a** are reported in Figure 1), the selectivity of the oxidation being dependent from the reaction solvent, substitution pattern [27,28], flow conditions [29], and photosensitizer properties. The synthesis of DHED by multi-step chrysazine-triggered photo-oxygenation in the presence of 1,8-dihydroxyanthraquinone (1,8-HOAQ) and PPh₃ has been also reported [30].

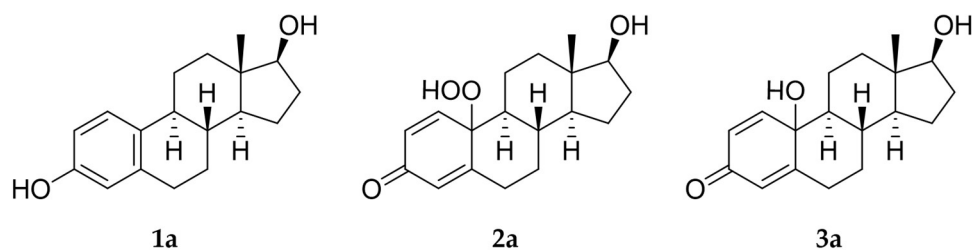
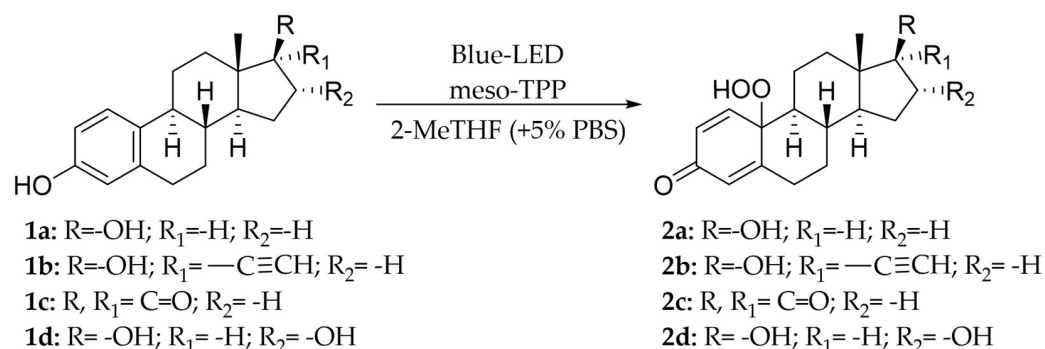


Figure 1. Structures of 17β-estradiol **1a**, hydro-peroxide **2a** and 10β, 17β-dihydroxyestra-1,4-dien-3-one (DHED) **3a**.

Recently, we described that singlet oxygen produced from blue-LED irradiation of meso-tetraphenyl porphyrin (meso-TPP) can be trapped by 2-methyltetrahydrofuran (2-MeTHF), favoring the oxidative coupling of phenols by Horseradish Peroxidase (HRP) [31]. This procedure avoided the inactivation of HRP by excess H₂O₂, working under experimental conditions simpler than those for in situ reduction of dioxygen [32–36]. Here, we describe the application of this procedure in the synthesis of estrogen-related hydroperoxide and quinol derivatives. The reaction solvent, photosensitizer, and buffer solution have been optimized in order to obtain high conversion of substrate and yield of the desired product.

2. Results and Discussion

17α-Ethinylestradiol **1b** was first studied as a model substrate. Compound **1b** (0.2 mmol) was dissolved in 2-MeTHF (32 mL) in the presence of meso-TPP (1.0 mol% with respect to substrate), followed by the addition of HRP (407 U) in sodium phosphate buffer (PBS; 16 mL 0.1 M, pH 6.0). The solution was gently stirred (200 rpm) under blue-LED irradiation (blue-LED stripes, 470 nm) and air atmosphere for 24 h at 28 °C. The photoreactor consisted of an internal jar (4.5 cm diameter) inserted in a supplementary external jar (7.5 cm diameter), and blue-LED strips were wrapped around the external jar and covered by aluminum foil (Figure S1). Under these experimental conditions, the hydro-peroxide **2b** was isolated as the only recovered product in low yield, besides the unreacted substrate (Scheme 1; Table 1, entry 1). No trace amounts of dimeric products, possibly derived from oxidative radical homo-coupling processes, were detected in the reaction mixture. The structure of hydro-peroxide **2b** was confirmed by spectroscopic and spectrometric analyses (including 2D NMR analysis; SI-Section 8), and by comparison with data previously reported [37].



Scheme 1. Blue LED-driven two-liquid-phase photo-oxygenation of estrogens **1a–d** to hydroperoxides **2a–d**.

When the reaction was carried out in the absence of HRP, the hydro-peroxide **2b** was again obtained as the only recovered product in acceptable yield, suggesting that the enzyme was not involved in the oxidation of the substrate (Table 1, entry 2). In addition, compound **1b** was unreactive when the reaction was carried out in the absence of buffer

(Table 1, entry 3), under dark conditions (Table 1, entry 4), and without meso-TPP (Table 1, entry 5) highlighting the key role played by blue-photons, pH, and photosensitizer in the transformation.

The activity of meso-TPP was compared with that of other useful photosensitizers, such as tris(2-phenyl-pyridine) iridium [Ir(ppy)₃] and Rose Bengal (structure and UV-vis adsorption spectra of the photosensitizers are in Figures S7–S9). As reported in Table 1, meso-TPP showed the highest activity in the photo-oxygenation of compound **1b** (entry 2 versus entries 6 and 7).

Table 1. Blue LED-driven two-liquid-phase photo-oxygenation of 17 α -ethinylestradiol **1b** to hydro-peroxide **2b**.

Entry	Light	Solvents	Photosensitizer (1.0 mol%)	Conversion ^a (%)	Yield ^a (%)
1	Blue-LED	2-MeTHF:PBS (2:1)	meso-TPP	20	12
2^b	Blue-LED	2-MeTHF:PBS (2:1)	meso-TPP	20	13
3	Blue-LED	2-MeTHF	meso-TPP	-	-
4	Dark	2-MeTHF:PBS (2:1)	meso-TPP	-	-
5	Blue-LED	2-MeTHF:PBS (2:1)	-	-	-
6	Blue-LED	2-MeTHF:PBS (2:1)	Ir(ppy) ₃	18	10
7	Blue-LED	2-MeTHF:PBS (2:1)	Rose Bengal	19	2

^a Conversion of substrate and yield of product were calculated on the basis of starting mmol of substrate; ^b Reaction performed under similar experimental conditions in the absence of HRP.

The possible formation of 2-MeTHF hydro-peroxide from 2-MeTHF during blue LED irradiation, previously observed by us [31], was evaluated by the pyrogallol assay at different reaction times (1, 2, 4, 6, and 24 h) and in the presence—or alternatively in the absence—of compound **1b**. As reported in Figure S2, compound **1b** lowered the concentration of 2-MeTHF hydro-peroxide, suggesting higher reactivity of compound **1b** with singlet oxygen with respect to the organic solvent. To optimize the photo-oxygenation procedure we analyzed the effect played by the concentration of substrate, the amount of the buffer (and relative pH), and the nature of the reaction solvent, on the process. Correspondingly to the other experimental parameters, hydro-peroxide **2b** was obtained in higher yield starting from 60 mM of substrate (Table 2, entry 1). This result was in accordance with the effect played by the concentration of the substrate on the intensity of the blue LED-photons in the bulk of the solution [38]. The high yield of hydro-peroxide **2b** was retained in the presence of a low amount of buffer (160 μ L, 5% *v/v* with respect to 2-MeTHF) (Table 2, entry 2) at pH 6, while it decreased at pH 8 (5% NaHCO₃ ss; Table 2, entry 3), and at pH 2 (AcOH 0.5%; Table 2, entry 4). Finally, we studied the effect of a panel of reaction solvents, characterized by a different stabilization effect for singlet oxygen, including CH₂Cl₂, EtOAc, and HFIP [39]. The highest yield of hydro-peroxide **2b** was obtained in CH₂Cl₂ (>98%; Table 2, entry 6) confirming the high stabilizing effect previously reported (Table 2, entry 6 versus entries 2, 5 and 7) [40]. The general order of reactivity was as follows: CH₂Cl₂ > 2-MeTHF > HFIP > EtOAc.

Next, we studied the photo-oxygenation of 17 β -estradiol **1a**, estrone **1c**, and estriol **1d** under optimal experimental conditions (that is: 60 mM of substrate, CH₂Cl₂, PBS, and meso-TPP). Unfortunately, estradiol **1a** and estriol **1d** showed very low conversion of substrate due to the limited solubility of CH₂Cl₂, while hydro-peroxide **2c** was obtained in quantitative conversion of the substrate and yield of the product (Table 3, entry 1).

Table 2. Optimization experiments for the synthesis of hydro-peroxide **2b**^a.

Entry	Solvents	Conversion ^b	Yield ^b (%)
1^c	2-MeTHF-PBS (2:1)	90	87
2^c	2-MeTHF (+5% PBS)	90	85
3^d	2-MeTHF (+5% NaHCO ₃ ss)	48	40

Table 2. Cont.

Entry	Solvents	Conversion ^b	Yield ^b (%)
4 ^e	2-MeTHF (+5% AcOH aq.0.5%)	38	32
5 ^c	EtOAc (+5% PBS)	65	56
6 ^c	CH ₂ Cl ₂ (+5% PBS)	>98	>98
7 ^c	HFIP (+5% PBS)	86	74

^a The reaction was performed solubilizing **1b** (0.2 mmol) and meso-TPP (1.0 mol%) in the organic solvent (3.2 mL) followed by the addition of the PBS. The solution was gently stirred (200 rpm) under blue-LED irradiation (blue-LED stripes, 470 nm) at 28 ± 1 °C for 24 h. ^b Conversion of substrate and yield of product were calculated on the basis of starting mmol of substrate; ^c PBS (0.1 M, pH 6); ^d NaHCO₃ saturated aqueous solution (pH 8); ^e AcOH 0.5% aqueous solution (pH 2).

The reaction was successively repeated in the second most reactive organic solvent previously observed in the oxidation of compound **1b**, 2-MeTHF, also taking advantage of its sustainability [35,36]. Under these experimental conditions, hydro-peroxides **2a** and **2c–d** were obtained, ranging from acceptable to high yields (Table 3, entry 2 and entries 4–5).

Table 3. Substrate scope of novel blue LED-driven two-liquid- phase photo-oxygenation^a.

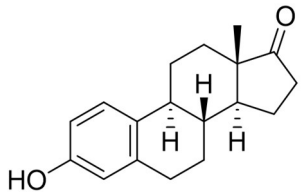
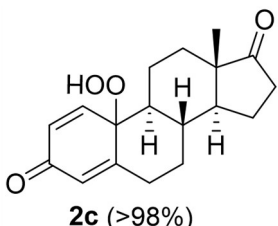
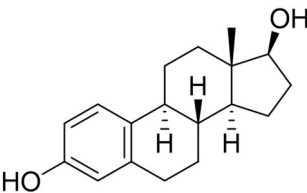
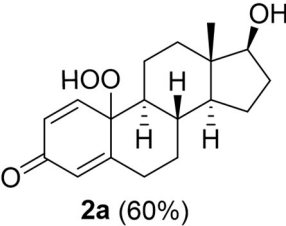
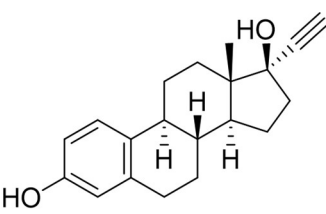
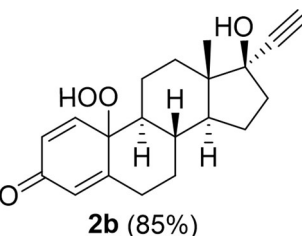
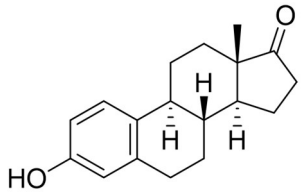
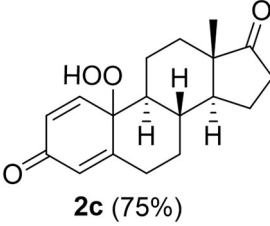
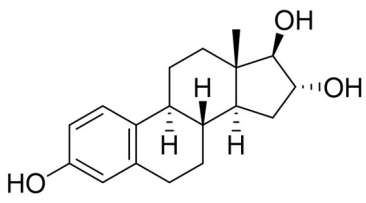
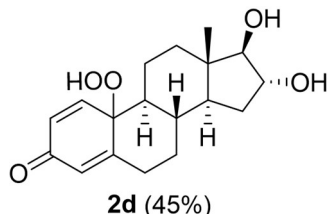
Entry	Cpd	Structure	Conversion ^b (%)	Product ^b (%)
1 ^c	1c		>98%	 2c (>98%)
2	1a		65	 2a (60%)
3	1b		90	 2b (85%)
4	1c		80	 2c (75%)

Table 3. Cont.

Entry	Cpd	Structure	Conversion ^b (%)	Product ^b (%)
5	1d		50	

^a The reaction was performed solubilizing compound **1** (0.2 mmol) and meso-TPP (1.0 mol%) in 2-MeTHF (3.2 mL), followed by the addition of PBS (160 μ L; 0.1M, pH 6). The solution was gently stirred (200 rpm) under blue-LED irradiation (blue-LED stripes, 470 nm) at 28 ± 1 °C for 24 h; ^b Conversion of substrate and yield of reaction product were calculated on the basis of starting mmol of substrate; ^c Reaction performed in CH_2Cl_2 .

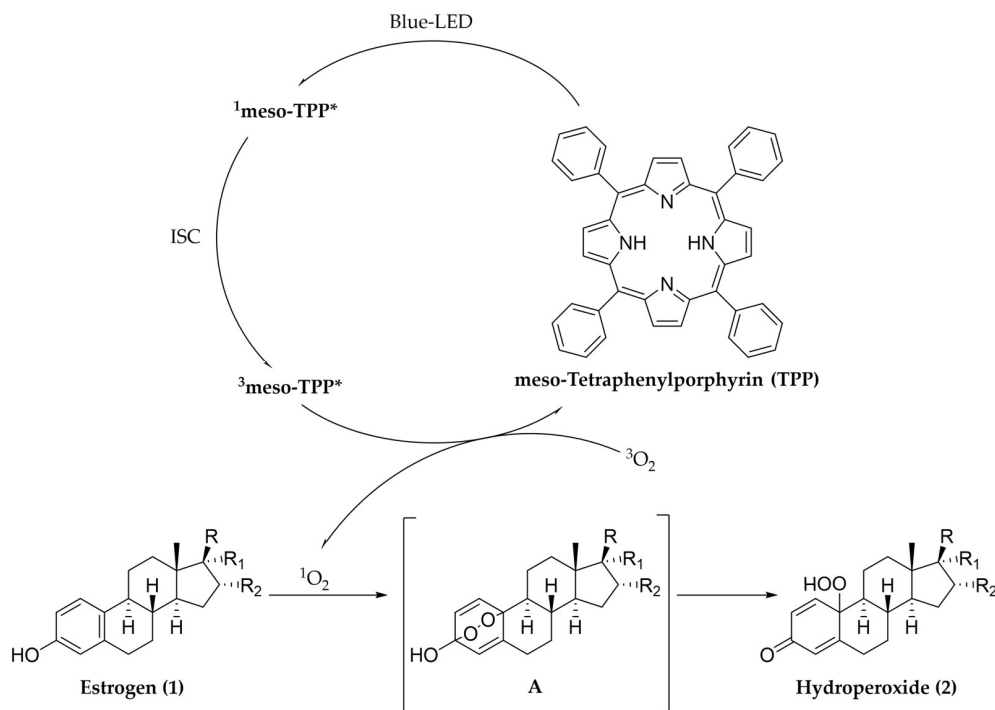
The mechanism of dye-mediated photo-oxygenation of phenols has been reviewed and discussed; it includes the transfer of the excited state from the photosensitizer to the substrate (Type I mechanism), or alternatively the inter-crossing system between the photosensitizer and dioxygen, with formation of singlet oxygen ($^1\text{O}_2$) (Type II mechanism) [38,41–43]. Under our experimental conditions, the Type I mechanism was most probably not operating, as suggested by the loss of reactivity of the substrate in the absence of meso-TPP (Table 1, entry 5), associated with the low absorption coefficient of estrogens in the interaction with blue-LED photons (Figures S3–S6) [44–47]. Additional experiments were performed to investigate the possible involvement of the Type II mechanism [43,48]. Hydroxy and superoxide radicals were not produced during the reaction as evaluated by the “coumarin” assay [48–51] (Figure S10) and the TEMPO assay (Figure S11) [52], respectively, while the NaN_3 assay (Figure S12) confirmed the involvement of $^1\text{O}_2$ [53–55]. In addition, the reaction was not effective under an argon atmosphere in the presence of degassed solvents (SI-Section 6). Although the possibility of the Type I mechanism cannot be completely ruled out, these data support the formation of $^1\text{O}_2$ as the primary oxidant in the photo-oxygenation of estrogens **1a–d**. This result is in accordance with the reported ability of meso-TPP to produce $^1\text{O}_2$ in aerated systems [42,43].

The tentative reaction pathway for the photo-oxygenation of compounds **1a–d** is reported in Scheme 2, it includes: (i) blue-LED photo-activation of meso-TPP to form the singlet excited state ($^1\text{meso-TPP}^*$); (ii) intersystem crossing (ISC) to form the triplet excited state ($^3\text{meso-TPP}^*$); (iii) energy transfer, and formation of singlet oxygen ($^1\text{O}_2$); (iv) selective insertion of $^1\text{O}_2$ on substrate to yield an unstable adduct **A** (not isolated in our case); and (v) rearrangement of adduct **A** to yield the corresponding hydro-peroxide.

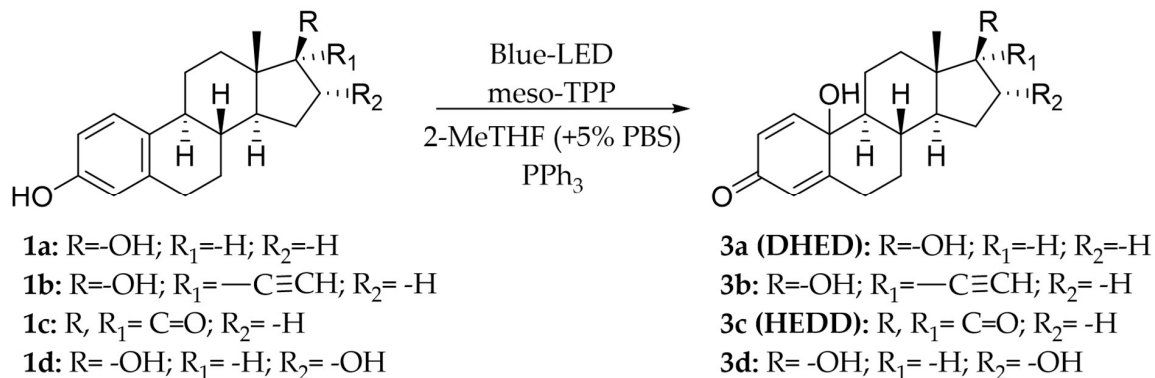
The reduction of hydro-peroxide **2b** was performed with different redox agents, $\text{Na}_2\text{S}_2\text{O}_3$, KI, and PPh_3 . In this latter case, the progress of the reduction was monitored by the analysis of the C-10 signal (81.020 ppm) in the ^{13}C NMR spectrum of the substrate, due to the high structural similarity between compound **2b**, and the corresponding quinol derivative **3b** (experimental procedures are in SI-Section 7). Among the reagents studied, PPh_3 afforded quinol **3b** in quantitative yield and conversion of substrate. PPh_3 was then used for the design of a novel one-pot synthesis of quinol **3b** by contemporary oxidation of 17α -ethinylestradiol **1b**, and in situ reduction of hydro-peroxide **2b** (Scheme 3).

Compound **1b** (60 mM) and meso-TPP (1.0 mol% with respect to substrate) were dissolved in 2-MeTHF, followed by addition of PBS (0.1M, pH 6; 5% with respect to organic solvent). The solution was gently stirred under blue-LED irradiation at 28 °C, and PPh_3 was added to the reaction mixture at indicated reaction times. The presence of PPh_3 at the starting point of the reaction totally inhibited the formation of quinol **3b**, with hydro-peroxide **2b** being the only recovered product (Table 4, entry 1), probably due to the fast oxidation of PPh_3 to triphenyl-phosphinoyl (TPPO). A better result was obtained when PPh_3 was added to the reaction mixture after 2 h. In this latter case, quinol **3b** was obtained with 50% yield and 70% conversion of substrate (Table 4, entry 2). The addition of PPh_3

after 3 h further increased the yield of quinol **3b**, and conversion of substrate (Table 4, entry 3). Longer addition times (e.g., 24 h) did not further increase the yield of quinol **3b** (Table 4, entry 4).



Scheme 2. Tentative reaction pathway for the photo-oxygenation of estrogen **1** by blue-LED irradiation in the presence of meso-TPP and bi-phasic system. “*” represents the excited structure of meso-TPP.



Scheme 3. One-pot synthesis of quinols **3a–d**.

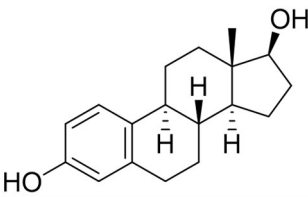
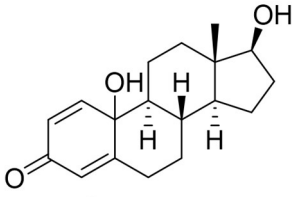
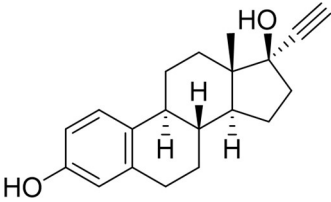
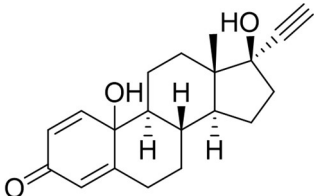
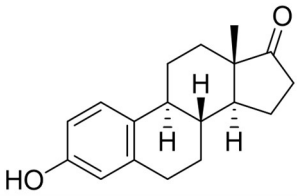
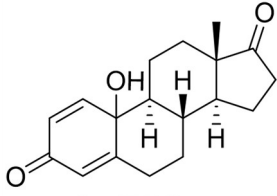
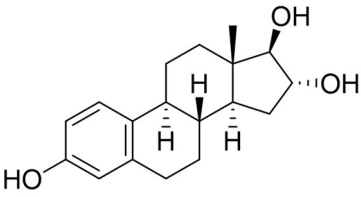
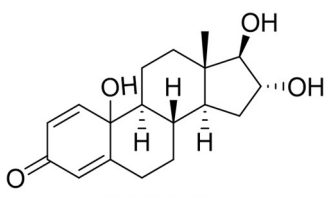
Table 4. One-pot synthesis of quinol **3b** at different times of addition of PPh₃ ^a.

Entry	Addition Time (h)	Reaction Time (h)	Conversion ^b (%)	Yield ^b (%)
1	0	24	15	10 ^c
2	2	24	70	50
3	3	24	90	84
4	24	48	90	88

^a The reaction was performed solubilizing **1b** (0.2 mmol) and meso-TPP (1.0 mol%) in 2-MeTHF (3.2 mL), followed by the addition of PBS (0.1 M, pH 6) and of PPh₃ (0.3 mmol) at different reaction times. The solution was gently stirred (200 rpm) under blue-LED irradiation (blue-LED stripes, 470 nm) at 28 ± 1 °C; ^b Conversion of substrate and yield of quinol **3b** were calculated on the basis of mmol of starting substrate. ^c Yield of hydroperoxide **2b**.

The one-pot procedure was then applied to estrogens **1a** and **1c–d** assuming 3 h as the optimal reaction time for the addition of PPh_3 . As reported in Table 5, quinols **3a** and **3c–d** were obtained ranging from acceptable to high yield (Table 5, entry 1 and entries 3–4). Quinols **3a** (DHED) and **3c** (HEDD) are well recognized pro-drugs in Hormone Replacement Therapy [9–14].

Table 5. Substrate scope of novel blue LED-driven two-liquid-phase in One-Pot condition ^a.

Entry	Cpd	Structure	Conversion ^b (%)	Product ^b (%)
1	1a		66	 3a (62%)
2	1b		89	 3b (84%)
3	1c		83	 3c (73%)
4	1d		53	 3d (46%)

^a The reaction was performed solubilizing **1a–d** (0.2 mmol) and meso-TPP (1.0 mol%) in 2-MeTHF (3.2 mL) and finally adding PBS (160 μL ; 0.1M, pH 6). The solution was gently stirred (200 rpm) under blue-LED irradiation (blue-LED stripes, 470 nm) at 28 ± 1 °C. After 3 h, the PPh_3 (0.3 mmol) was added to the reaction mixture; ^b Conversion of substrate and yield of reaction product were calculated on the basis of mmol of starting substrate.

3. Materials and Methods

3.1. General Considerations

Commercially available reagents were used without further purification. Chromatographic separations were performed on Merck silica gel 60 (230–400 mesh). R_f values are referred to TLC carried out on 0.25 mm silica gel plates (F254) using the eluent indicated for column chromatography. All products were dried in high vacuum (10–3 mbar) before characterization. ¹H NMR, ¹³C NMR, and 2D NMR were recorded on a Bruker Advance DRX400 (400 MHz/100 MHz) spectrometer. Chemical shifts are in parts per million (δ scale) and internally referenced the CD_3OD signal at δ 3.31 and 49.00 ± 0.01 ppm, respectively. Coupling constants (J) are reported in Hz. UV-visible (UV-vis) spectra were recorded using Cary 60 UV-Vis spectrophotometer, Agilent, Santa Clara, USA. Blue-LED apparatus

consisted of a 1.0 m blue-LED strip (wavelength 470 nm, nominal capacity/m 14.4 W) LEDXON MODULAR 9009083 LED.

3.2. General Procedure for the Synthesis of Hydro-Peroxides 2a–d

The selected estrogen (0.2 mmol) and meso-TPP (1 mol%) were dissolved in 2-Me-THF (3.2 mL), followed by the addition of PBS (0.16 mL; 0.1 M, pH 6), and the mixture was gently stirred (200 rpm) under blue-LED irradiation and air atmosphere at 28 ± 1 °C for 24 h. The reaction mixture was washed with brine (3×2 mL), dried over sodium sulphate, and evaporated under vacuum. The crude mixture was purified by column chromatography.

10-hydroperoxy-17-hydroxy-13-methyl-6,7,8,9,10,11,12,13,14,15,16,17-dodecahydro-3H-cyclopenta[a]phenanthren-3-one (**2a**):

$R_f = 0.18$ (PE:AcOEt 1:1); oil (yield 60%). $^1\text{H NMR}$ (400 MHz, CD_3OD): $\delta = 7.31$ (d, $J = 10.4$ Hz, 1H), 6.24 (dd, $J = 8, 2.1$ Hz, 1H), 6.10 (s, 1H), 3.56 (t, $J = 8.4$ Hz, 1H), 2.80–2.71 (m, 1H), 2.41 (ddd, $J = 12.4, 4.2, 2.3$ Hz, 1H), 2.03–1.81 (m, 5H), 1.76–1.66 (m, 1H), 1.66–1.56 (m, 1H), 1.53–1.44 (m, 1H), 1.34 (qd, $J = 12.2, 5.8$ Hz, 1H), 1.14–0.92 (m, 4H), 0.80 (s, 3H). $^{13}\text{C NMR}$ (100 MHz, CD_3OD): $\delta = 186.6$ (C3), 166.9 (C5), 151.9 (C1), 129.4 (C2), 123.9 (C4), 81.1 (C17), 80.6 (C10), 55.6 (C9), 49.9 (C14), 42.8 (C13), 36.2 (C12), 35.4 (C8), 33.3 (C7), 31.7 (C6), 29.1 (C16), 23.0 (C15), 22.7 (C11), 10.0 (C18) ppm; ESIMS m/z 327.1 $[\text{M} + \text{Na}]^+$. The spectral data were in accordance with the results previously reported [26].

17-ethynyl-10-hydroperoxy-17-hydroxy-13-methyl-6,7,8,9,10,11,12,13,14,15,16,17-dodecahydro-3H-cyclopenta[a]phenanthren-3-one (**2b**):

$R_f = 0.23$ (PE:AcOEt 3:2); oil (yield 85%). $^1\text{H NMR}$ (400 MHz, CD_3OD): $\delta = 7.317$ (d, $J = 10$ Hz, 1H), 6.29 (dd, $J = 8, 2$ Hz, 1H), 6.11 (s, 1H), 2.86 (s, 1H), 2.81–2.80 (m, 1H), 2.43–2.40 (m, 1H), 2.21–2.20 (m, 1H), 2.04–1.86 (m, 5H), 1.73–1.66 (m, 3H), 1.49–1.37 (m, 2H), 1.23–1.22 (m, 1H), 1.19–1.06 (m, 1H), 0.89 (s, 3H) ppm. $^{13}\text{C NMR}$ (100 MHz, CD_3OD): $\delta = 186.6$ (C3), 166.7 (C5), 151.8 (C1), 129.5 (C2), 124.0 (C4), 87.0 (C20), 81.0 (C10), 78.6 (C17), 73.4 (C21), 55.2 (C9), 49.4 (C14), 46.6 (C15), 38.2 (C8), 36.0 (C16), 33.4 (C6), 32.3 (C12), 31.6 (C7), 22.7 (C11), 11.6 (C18) ppm. ESIMS m/z 351.1 $[\text{M} + \text{Na}]^+$. The spectral data were in accordance with the results previously reported [26].

10-hydroperoxy-13-methyl-7,8,9,10,11,12,13,14,15,16-decahydro-3H-cyclopenta[a]phenanthrene-3,17(6H)-dione (**2c**):

$R_f = 0.21$ (PE:AcOEt 3:2); oil (yield 75%). $^1\text{H NMR}$ (400 MHz, CD_3OD): $\delta = 7.30$ (d, $J = 10$, 1H), 6.30 (dd, $J = 8.4, 2$, 1H), 6.13 (s, 1H), 2.85–2.84 (m, 1H), 2.49–2.42 (m, 2H), 2.17–1.90 (m, 6H), 1.81–1.76 (m, 1H), 1.68–1.62 (m, 1H), 1.38–1.18 (m, 4H), 0.94 (s, 3H) ppm. $^{13}\text{C NMR}$ (100 MHz, CD_3OD): $\delta = 221.4$ (C17), 186.5 (C3), 166.3 (C5), 151.5 (C1), 129.6 (C2), 124.1 (C4), 80.9 (C10), 55.0 (C9), 50.0 (C14), 35.0 (C15), 34.9 (C8), 32.4 (C16), 31.4 (C6), 30.9 (C12), 22.1 (C7), 21.4 (C11), 12.6 (C18) ppm. ESIMS m/z 325.1 $[\text{M} + \text{Na}]^+$. The spectral data were in accordance with the results previously reported [37].

10-hydroperoxy-16,17-dihydroxy-13-methyl-6,7,8,9,10,11,12,13,14,15,16,17-dodecahydro-3H-cyclopenta[a]phenanthren-3-one (**2d**):

$R_f = 0.26$ (CH_2Cl_2 :MeOH 30:3); oil (45%). $^1\text{H NMR}$ (400 MHz, CD_3OD): $\delta = 7.22$ (d, $J = 10.4$, 1H), 6.14 (dd, $J = 12.8, 2$, 1H), 5.98 (s, 1H), 4.03 (t, $J = 6, 7.2$, 1H), 2.79–2.78 (m, 1H), 2.35 (d, $J = 11.2$, 1H), 2.02–1.90 (m, 3H), 1.85–1.83 (m, 3H), 1.79–1.69 (m, 1H), 1.54–1.48 (m, 1H), 1.35–1.30 (m, 1H), 1.18–1.04 (m, 3H), 0.85 (s, 3H) ppm. $^{13}\text{C NMR}$ (100 MHz, CD_3OD): $\delta = 186.8$ (C3), 168.9 (C5), 153.5 (C1), 126.3 (C2), 121.4 (C4), 88.9 (C17), 78.7 (C10), 77.1 (C16), 55.3 (C9), 43.5 (C13), 36.1 (C12), 34.4 (C8), 33.9 (C7), 33.2 (C6), 31.7 (C15), 21.9 (C11), 11.2 (C18) ppm. ESIMS m/z 343.1 $[\text{M} + \text{Na}]^+$.

3.3. General Procedure for the Synthesis of Estrogen-Related Quinolins 3a–d

The selected estrogen (0.2 mmol) and meso-TPP (1.0 mol%) were dissolved in 2-Me-THF (3.2 mL), followed by the addition of PBS (0.16 mL; 0.1 M, pH 6), and the mixture was gently stirred (200 rpm) under blue-LED irradiation and air atmosphere at 28 ± 1 °C for 3 hrs. Then PPh_3 (0.3 mmol) was added, and the reaction was left under magnetic stirring for 21 h. After washing with brine (3×2 mL), the reaction mixture was dried

over sodium sulphate, and evaporated under vacuum. The crude mixture was purified by column chromatography.

10,17-dihydroxy-13-methyl-6,7,8,9,10,11,12,13,14,15,16,17-dodecahydro-3H-cyclopenta[a]phenanthren-3-one (**3a**, **DHED**):

$R_f = 0.17$ (CH_2Cl_2 :AcOEt 9:2.5); oil (yield 62%). ^1H NMR (400 MHz, CD_3OD): $\delta = 7.23$ (d, $J = 10.4$ Hz, 1H), 6.14 (dd, $J = 8, 2.1$ Hz, 1H), 5.97 (s, 1H), 3.58 (t, $J = 8.4$ Hz, 1H), 2.79–2.78 (m, 1H), 2.34 (ddd, $J = 12.4, 4.2, 2.3$ Hz, 1H), 2.04–1.73 (m, 5H), 1.76–1.66 (m, 1H), 1.706–1.56 (m, 1H), 1.53–1.44 (m, 1H), 1.34 (qd, $J = 12.2, 5.8$ Hz, 1H), 1.14–0.92 (m, 4H), 0.84 (s, 3H). ^{13}C NMR (100 MHz, CD_3OD): $\delta = 186.8$ (C3), 169.1 (C5), 153.7 (C1), 126.3 (C2), 121.3 (C4), 80.8 (C17), 69.72 (C10), 55.46 (C9), 49.7 (C14), 42.9 (C13), 36.2 (C12), 34.9 (C8), 33.3 (C7), 31.6 (C6), 29.1 (C16), 23.1 (C15), 22.3 (C11), 10.1 (C18) ppm. ESIMS m/z 311.1 $[\text{M} + \text{Na}]^+$. The spectral data were in accordance with the results previously reported [30].

17-ethynyl-10,17-dihydroxy-13-methyl-6,7,8,9,10,11,12,13,14,15,16,17-dodecahydro-3H-cyclopenta[a]phenanthren-3-one (**3b**):

$R_f = 0.18$ (CH_2Cl_2 :AcOEt 9:1); oil (yield 84%). ^1H NMR (400 MHz, CD_3OD): $\delta = 7.31$ (d, $J = 10$ Hz, 1H), 6.29 (dd, $J = 8, 2$ Hz, 1H), 6.11 (s, 1H), 2.86 (s, 1H), 2.81–2.80 (m, 1H), 2.43–2.40 (m, 1H), 2.21–2.20 (m, 1H), 2.04–1.86 (m, 5H), 1.73–1.66 (m, 3H), 1.49–1.37 (m, 2H), 1.23–1.22 (m, 1H), 1.19–1.06 (m, 1H), 0.89 (s, 3H) ppm. ^{13}C NMR (100 MHz, CD_3OD): $\delta = 186.8$ (C3), 168.9 (C5), 153.5 (C1), 126.3 (C2), 121.4 (C4), 87.2 (C20), 78.7 (C17), 73.4 (C21), 69.6 (C10), 55.1 (C9), 49.2 (C14), 46.7 (C13), 38.3 (C15), 35.5 (C8), 33.3 (C16), 32.2 (C6), 31.7 (C12), 22.8 (C7), 22.3 (C11), 11.7 (C18) ppm. ESIMS m/z 335.1 $[\text{M} + \text{Na}]^+$. The spectral data were in accordance with the results previously reported [56].

10-hydroxy-13-methyl-7,8,9,10,11,12,13,14,15,16-decahydro-3H-cyclopenta[a]phenanthrene-3,17(6H)-dione (**3c**, **HEDD**):

$R_f = 0.36$ (PE:AcOEt 1:1); oil (yield 73%). ^1H NMR (400 MHz, CD_3OD): $\delta = 7.23$ (d, $J = 10$, 1H), 6.15 (dd, $J = 8.4, 2$, 1H), 6.00 (s, 1H), 2.84–2.83 (m, 1H), 2.48–2.39 (m, 2H), 2.19–1.97 (m, 6H), 1.83–1.79 (m, 1H), 1.69–1.63 (m, 1H), 1.39–1.12 (m, 4H), 0.98 (s, 3H) ppm. ^{13}C NMR (100 MHz, CD_3OD): $\delta = 221.8$ (C17), 186.7 (C3), 168.5 (C5), 153.2 (C1), 126.5 (C2), 121.5 (C4), 69.5 (C10), 55.0 (C9), 49.8 (C14), 35.1 (C15), 34.4 (C8), 32.3 (C16), 31.5 (C6), 30.9 (C12), 21.8 (C7), 21.5 (C11), 12.7 (C18) ppm. ESIMS m/z 309.1 $[\text{M} + \text{Na}]^+$. The spectral data were in accordance with the results previously reported [57].

10,16,17-trihydroxy-13-methyl-6,7,8,9,10,11,12,13,14,15,16,17-dodecahydro-3H-cyclopenta[a]phenanthren-3-one (**3d**):

$R_f = 0.26$ (CH_2Cl_2 :MeOH 30:3); oil (yield 46%). ^1H NMR (400 MHz, CD_3OD): $\delta = 7.22$ (d, $J = 10.4$, 1H), 6.14 (dd, $J = 12.8, 2$, 1H), 5.98 (s, 1H), 4.03 (t, $J = 6, 7.2$, 1H), 2.79–2.78 (m, 1H), 2.35 (d, $J = 11.2$, 1H), 2.02–1.90 (m, 3H), 1.85–1.83 (m, 3H), 1.79–1.69 (m, 1H), 1.54–1.48 (m, 1H), 1.36–1.30 (m, 1H), 1.18–1.04 (m, 3H), 0.86 (s, 3H) ppm. ^{13}C NMR (100 MHz, CD_3OD): $\delta = 186.8$ (C3), 168.9 (C5), 153.5 (C1), 126.3 (C2), 121.4 (C4), 88.9 (C17), 77.1 (C16), 69.6 (C10), 55.3 (C9), 48.4 (C14), 43.5 (C13), 36.1 (C12), 34.4 (C8), 33.9 (C7), 33.2 (C6), 31.7 (C15), 21.9 (C11), 11.2 (C18) ppm. ESIMS m/z 327.1 $[\text{M} + \text{Na}]^+$.

4. Conclusions

In conclusion, we developed a novel one-pot approach for the synthesis of estrogen-related quinols by using blue LED-driven photo-oxygenation in a two-liquid-phase system. The reaction proceeded under mild and sustainable conditions, including with a catalytic amount of meso-TPP, eco-certified 2-MeTHF, and buffer as solvents, and PPh_3 as the reducing agent. The reaction pathway involved blue-LED photo-activation of meso-TPP, and the generation of singlet oxygen ($^1\text{O}_2$) (Type II mechanism), followed by oxidation of estrogen to the corresponding hydro-peroxide, and in situ reduction of hydro-peroxide to the desired quinol. Under these experimental conditions, quinols were synthesized ranging from acceptable to very high yield, including two well recognized pro-drugs in Hormone Replacement Therapy, DHED and HEDD. The irrelevance of the Type I mechanism was suggested by the un-reactivity of the system, in the absence of the photosensitizer associated

with the low adsorption capacity of estrogens towards blue-LED photons. The presence of 2-MeTHF hydro-peroxide, OH, and superoxide radicals in the reaction pathway was investigated, and ruled-out by means of different specific assays. The additional scopes and applications of this photocatalytic process will be further investigated in our laboratory.

Supplementary Materials: The following supporting information can be downloaded at: <https://www.mdpi.com/article/10.3390/molecules27248961/s1>, Reaction set up; 2-Me-THF hydroperoxide assay; UV-visible analysis; Coumarin assay; Quenching experiments; degassed conditions; Screening of reducing agents; 1D and 2D NMR spectra. Figure S1: reaction set up; Figure S2: 2-MeTHF hydroperoxide assay; Figure S3–S6: estrogens UV-visible spectra; Figures S7–S9: photosensitizers UV-visible spectra; Figure S10: coumarin assay; Figure S11: photo-oxygenation of **1c** in presence of TEMPO as radical scavenger; Figure S12: photo-oxygenation of **1c** in presence of NaN₃ as singlet oxygen scavenger; Figure S13: photo-oxygenation of **1b** under degassed conditions; Figure S14: reduction of hydroperoxide **2b** by Na₂S₂O₃; Figure S15: reduction of hydroperoxide **2b** by KI; Figure S16: reduction of hydroperoxide **2b** by PPh₃; Figures S17–S28: ¹H NMR, ¹³C NMR and 2D NMR spectra of hydro-peroxides **2a–d**; Figures S29–S36: ¹H NMR and ¹³C NMR spectra of quinols **3a–d**.

Author Contributions: Conceptualization, L.B. and R.S.; methodology, E.D.M.; investigation, E.D.M. and B.M.B.; writing—original draft preparation, E.D.M.; writing—review and editing, R.S. All authors have read and agreed to the published version of the manuscript.

Funding: This research was funded by Ministero dell’Istruzione, dell’Università della Ricerca Italiano (MIUR), PRIN 2017, ORIGINALE CHEMIAE in Antiviral Strategy—Origin and Modernization of Multi-Component Chemistry as a Source of Innovative Broad Spectrum Antiviral Strategy, cod. 2017BMK8JR.

Institutional Review Board Statement: Not applicable.

Informed Consent Statement: Not applicable.

Data Availability Statement: Not applicable.

Acknowledgments: The Centro Grandi Apparecchiture CGA of the University of Tuscia is acknowledged.

Conflicts of Interest: The authors declare no conflict of interest.

References

1. Gruber, C.J.; Tschugguel, W.; Schneeberger, C.; Huber, J.C. Production and Actions of Estrogens. *N. Engl. J. Med.* **2002**, *346*, 340–352. [[CrossRef](#)]
2. Lobo, R.A. Hormone-replacement therapy: Current thinking. *Nat. Rev. Endocrinol.* **2017**, *13*, 220–231. [[CrossRef](#)] [[PubMed](#)]
3. Prokai, L.; Prokai, K.; Simpkins, J. Preparation of Steroidal Quinols and Their Use for Estrogen Replacement Therapy. U.S. Patent US7300926B2, 27 November 2007.
4. Lobo, R.A. Benefits and risks of estrogen replacement therapy. *Am. J. Obstet. Gynecol.* **1995**, *173*, 982–989. [[CrossRef](#)] [[PubMed](#)]
5. D’Alonzo, M.; Bounous, V.E.; Villa, M.; Bigli, N. Current evidence of the oncological benefit-risk profile of hormone replacement therapy. *Medicina* **2019**, *55*, 573. [[CrossRef](#)]
6. Cushman, M.; Larson, J.C.; Rosendaal, F.R.; Heckbert, S.R.; Curb, J.D.; Phillips, L.S.; Baird, A.E.; Eaton, C.B.; Stafford, R.S. Biomarkers, menopausal hormone therapy and risk of venous thrombosis: The Women’s Health Initiative. *Res. Pract. Thromb. Haemost.* **2018**, *17*, 310–319. [[CrossRef](#)] [[PubMed](#)]
7. Bassuk, S.S.; Manson, J.E. The timing hypothesis: Do coronary risks of menopausal hormone therapy vary by age or time since menopause onset. *Metab. Clin. Exp.* **2016**, *65*, 794–803. [[CrossRef](#)]
8. Prokai-Tatrai, K.; Prokai, L. A Novel Prodrug Approach for Central Nervous System-Selective Estrogen Therapy. *Molecules* **2019**, *24*, 4197–4214. [[CrossRef](#)]
9. Prokai, L.; Nguyen, V.; Szarka, S.; Garg, P.; Sabnis, G.; Bimonte-Nelson, H.A.; McLaughlin, K.J.; Talboom, J.S.; Conrad, C.D.; Shugrue, P.J.; et al. The prodrug DHED selectively delivers 17β-estradiol to the brain for treating estrogen-responsive disorders. *Sci. Transl. Med.* **2015**, *7*, 297ra113. [[CrossRef](#)]
10. Prokai-Tatrai, K.; Nguyen, V.; De La Cruz, D.L.; Guerra, R.; Zaman, K.; Rahlouni, F.; Prokai, L. Retina-Targeted Delivery of 17β-Estradiol by the Topically Applied DHED Prodrug. *Pharmaceutics* **2020**, *12*, 456–468. [[CrossRef](#)]
11. Prokai-Tatrai, K.; Zaman, K.; Nguyen, V.; De La Cruz, D.L.; Prokai, L. Proteomics-Based Retinal Target Engagement Analysis and Retina-Targeted Delivery of 17β-Estradiol by the DHED Prodrug for Ocular Neurotherapy in Males. *Pharmaceutics* **2021**, *13*, 1392–1409. [[CrossRef](#)]

12. Merchenthaler, I.; Lane, M.; Stennett, C.; Zhan, M.; Nguyen, V.; Prokai-Tatrai, K.; Prokai, L. Brain-Selective Estrogen Therapy Prevents Androgen Deprivation-Associated Hot Flushes in a Rat Model. *Pharmaceuticals* **2020**, *13*, 119–129. [[CrossRef](#)] [[PubMed](#)]
13. Tschiffely, A.E.; Schuh, R.A.; Prokai-Tatrai, K.; Prokai, L.; Ottinger, M.A. A comparative evaluation of treatments with 17 β -estradiol and its brain-selective prodrug in a double-transgenic mouse model of Alzheimer's disease. *Horm. Behav.* **2016**, *83*, 39–44. [[CrossRef](#)] [[PubMed](#)]
14. Thadathil, N.; Xiao, J.; Hori, R.; Alway, S.E.; Khan, M.M. Brain Selective Estrogen Treatment Protects Dopaminergic Neurons and Preserves Behavioral Function in MPTP-induced Mouse Model of Parkinson's Disease. *J. Neuroimmune Pharm.* **2021**, *16*, 667–678. [[CrossRef](#)] [[PubMed](#)]
15. Quideau, S.; Pouységou, L.; Deffieux, D. Oxidative Dearomatization of Phenols: Why, How and What For? *Synlett* **2008**, *4*, 467–495. [[CrossRef](#)]
16. Baker Dockrey, S.A.; Lukowski, A.L.; Becker, M.R.; Narayan, A.R.H. Biocatalytic site- and enantioselective oxidative dearomatization of phenols. *Nat. Chem.* **2018**, *10*, 119–125. [[CrossRef](#)]
17. Roche, S.P.; Porco, J.A. Dearomatization Strategies in the Synthesis of Complex Natural Products. *Angew. Chem. Int. Ed.* **2011**, *50*, 4068–4093. [[CrossRef](#)]
18. Ding, Q.; Ye, Y.; Fan, R. Recent Advances in Phenol Dearomatization and Its Application in Complex Syntheses. *Synthesis* **2013**, *45*, 1–16. [[CrossRef](#)]
19. Bizzarri, B.M.; Fanelli, A.; Piccinino, D.; De Angelis, M.; Dolfa, C.; Palamara, A.T.; Nencioni, L.; Zippilli, C.; Crucianelli, M.; Saladino, R. Synthesis of Stilbene and Chalcone Inhibitors of Influenza A Virus by SBA-15 Supported Hoveyda-Grubbs Metathesis. *Catalysts* **2019**, *9*, 983–999. [[CrossRef](#)]
20. Sun, W.; Li, G.; Hong, L.; Wang, R. Asymmetric dearomatization of phenols. *Org. Biomol. Chem.* **2016**, *14*, 2164–2176. [[CrossRef](#)]
21. Wu, W.T.; Zhang, L.; You, S.L. Catalytic asymmetric dearomatization (CADA) reactions of phenol and aniline derivatives. *Chem. Soc. Rev.* **2016**, *45*, 1570–1580. [[CrossRef](#)]
22. Carreño, M.C.; González-López, M.; Urbano, A. Oxidative De-aromatization of *para*-Alkyl Phenols into *para*-Peroxyquinols and *para*-Quinols Mediated by Oxone as a Source of Singlet Oxygen. *Angew. Chem. Int. Ed.* **2006**, *45*, 2737–2741. [[CrossRef](#)] [[PubMed](#)]
23. Moriarty, R.M.; Prakash, O. Oxidation of Phenolic Compounds with Organohypervalent Iodine Reagents. *Org. React.* **2001**, *57*, 327–415. [[CrossRef](#)]
24. Parra, A.; Reboredo, S. Chiral Hypervalent Iodine Reagents: Synthesis and Reactivity. *Chem. Eur. J.* **2013**, *19*, 17244–17260. [[CrossRef](#)] [[PubMed](#)]
25. Sels, B.F.; De Vos, D.E.; Jacobs, P.A. Bromide-Assisted Oxidation of Substituted Phenols with Hydrogen Peroxide to the Corresponding *p*-Quinol and *p*-Quinol Ethers over WO₄²⁻-Exchanged Layered Double Hydroxides. *Angew. Chem. Int. Ed.* **2004**, *44*, 310–313. [[CrossRef](#)] [[PubMed](#)]
26. Lupon, P.; Gomez, J.; Bonet, J.J. Photo-oxygenation of Styrenic Estrogens: A New Synthesis of 19-Norsteroids. *Angew. Chem. Suppl.* **1983**, 1025–1034. [[CrossRef](#)]
27. Lupon, P.; Grau, F.; Bonet, J.J. The photooxygenation of $\Delta^{9(11)}$ -dehydroestrone and its 3-methyl ether photochemical reactions XX. Preliminary communication. *Helv. Chim. Acta* **1984**, *67*, 332–333. [[CrossRef](#)]
28. Planas, A.; Lupon, P.; Cascallo, M.; Bonet, J.J. Photo-oxygenation of Styrenic Estrogens: Product characterization and kinetics of the dye-sensitized photo-oxygenation of 9,11-didehydroestrone derivatives. *Helv. Chim. Acta* **1989**, *72*, 715–724. [[CrossRef](#)]
29. Wellauer, J.; Miladinov, D.; Buchholz, T.; Schutz, J.; Stemmler, R.T.; Medlock, J.A.; Bonrath, W.; Sparr, C. Organophotocatalytic Aerobic Oxygenation of Phenols in a Visible-Light Continuous-Flow Photoreactor. *Chem. Eur. J.* **2021**, *27*, 9748–9752. [[CrossRef](#)]
30. Afanasenko, A.; Kavun, A.; Thomas, D.; Li, C.J. A One-Pot Approach for Bio-Based Arylamines via a Combined Photooxidative Dearomatization-Rearomatization Strategy. *Chem. Eur. J.* **2022**, *28*, 1–7. [[CrossRef](#)]
31. Zippilli, C.; Bizzarri, B.M.; Gabellone, S.; Botta, L.; Saladino, R. Oxidative Coupling of Coumarins by Blue-LED-Driven in situ Activation of Horseradish Peroxidase in a Two-Liquid-Phase System ChemCatChem **2021**, *13*, 4151–4158. [[CrossRef](#)]
32. Bankar, S.B.; Bule, M.V.; Singhal, R.S.; Ananthanarayan, L. Glucose oxidase—An overview. *Biotechnol. Adv.* **2009**, *27*, 489–501. [[CrossRef](#)]
33. Tieves, F.; Willot, S.J.-P.; van Schie, M.M.C.H.; Rauch, M.C.R.; Younes, S.H.H.; Zhang, W.; Dong, J.; de Santos, P.; Robbins, J.M.; Bommarius, B.; et al. Formate Oxidase (FOx) from *Aspergillus oryzae*: One Catalyst Enables Diverse H₂O₂-Dependent Biocatalytic Oxidation Reactions. *Angew. Chem. Int. Ed.* **2019**, *58*, 7873–7877. [[CrossRef](#)] [[PubMed](#)]
34. Wapshott-Stehli, H.L.; Grunden, A.M. In situ H₂O₂ generation methods in the context of enzyme biocatalysis. *Enzym. Microb. Technol.* **2021**, *145*, 109744. [[CrossRef](#)] [[PubMed](#)]
35. Monticelli, S.; Castoldi, L.; Murgia, I.; Senatore, R.; Mazzeo, E.; Wackerlig, J.; Urban, E.; Langer, T.; Pace, V. Recent advancements on the use of 2-methyltetrahydrofuran in organometallic chemistry. *Monatsh. Chem.* **2017**, *148*, 37–48. [[CrossRef](#)] [[PubMed](#)]
36. Ismael, A.; Gevorgyan, A.; Skrydstrup, T.; Bayer, A. Renewable Solvents for Palladium-Catalyzed Carbonylation Reactions. *Org. Process Res. Dev.* **2020**, *24*, 2665–2675. [[CrossRef](#)]
37. Sedee, A.; van Henegouwen, G.B. Photosensitized Decomposition of Contraceptive Steroids: A Possible Explanation for the Observed (Photo)allergy of the Oral Contraceptive Pill. *Arch. Pharm.* **1985**, *318*, 111–119. [[CrossRef](#)]
38. Noyes, W.A.; Hammond, G.S.; Pittis, J.N. *Advances in Photochemistry*; Interscience Publishers: New York, NY, USA; London, UK; Sydney, Australia; pp. 1–483. 1968; Volume 6, pp. 1–483.

39. Wilkinson, F.; McGamey, D.J.; Olea, A.F. Factors governing the efficiency of singlet oxygen production during oxygen quenching of singlet and triplet states of anthracene derivatives in cyclohexane solution. *J. Am. Chem. Soc.* **1993**, *115*, 12144–12151. [[CrossRef](#)]
40. Wilkinson, F.; Ayman, A.A.-S. Mechanism of Quenching of Triplet States by Molecular Oxygen: Biphenyl Derivatives in Different Solvents. *J. Phys. Chem. A* **1999**, *103*, 5425–5435. [[CrossRef](#)]
41. Fischer, J.; Nun, P.; Coeffard, V. Visible-Light-Driven Transformations of Phenols via Energy Transfer. *Catal. Synth.* **2020**, *52*, 1617–1624. [[CrossRef](#)]
42. Buzzetti, L.; Crisenza, G.E.M.; Melchiorre, P. Mechanistic Studies in Photocatalysis. *Angew. Chem. Int. Ed.* **2019**, *58*, 3730–3747. [[CrossRef](#)]
43. Pfoertner, K.-H. Photochemistry. In *Ullmann's Encyclopedia of Industrial Chemistry*; Wiley: New York, NY, USA, 2000. [[CrossRef](#)]
44. Li, J.; Mailhot, G.; WuNansheng, F. Deng Photochemical efficiency of Fe(III)-EDDS complex: •OH radical production and 17β-estradiol degradation. *J. Photochem. Photobiol. A Chem.* **2010**, *212*, 1–7. [[CrossRef](#)]
45. Yamamoto, A.; Kodama, S.; Matsunaga, A.; Nakazawa, H.; Hayakawa, K. Fluorescence-Detected Circular Dichroism by Modulated Beam in the Wavelength Axial Direction. *A J. Stereochemistry* **2002**, *7*, 225–229. [[CrossRef](#)] [[PubMed](#)]
46. Soto, C.; Contreras, D.; Yez, J.; Otipka, R.; Toral, M.I.; Pino, D. Determination and co-estimate of the chlormadinone acetate and 17α-ethinyl estradiol in pharmaceutical formulation and drinking water samples by digital derivative spectrophotometry. *J. Chil. Chem. Soc.* **2014**, *59*, 2485–2489. [[CrossRef](#)]
47. Li, W.J.; Chang, L.; Liu, Q.; Ning, D.; Yao, X.Y.; Li, Y.; Ruan, W.J. Enzyme-Assisted Metal–Organic Framework Sensing System for Diethylstilbestrol Detection. *Eur. J. Chem.* **2017**, *23*, 15498–15504. [[CrossRef](#)]
48. Raghavan, N.V.; Steenken, S. Electrophilic reaction of the hydroxyl radical with phenol. Determination of the distribution of isomeric dihydroxycyclohexadienyl radicals. *J. Am. Chem. Soc.* **1980**, *102*, 3495–3499. [[CrossRef](#)]
49. Zhang, J.; Nosaka, Y. Quantitative Detection of OH Radicals for Investigating the Reaction Mechanism of Various Visible-Light TiO₂ Photocatalysts in Aqueous Suspension. *J. Phys. Chem. C* **2013**, *117*, 1383–1391. [[CrossRef](#)]
50. Maier, A.C.; Iglebaek, E.H.; Jonsson, M. Confirming the Formation of Hydroxyl Radicals in the Catalytic Decomposition of H₂O₂ on Metal Oxides Using Coumarin as a Probe. *ChemCatChem* **2019**, *11*, 5435–5438. [[CrossRef](#)]
51. Leandri, V.; Gardner, J.M.; Jonsson, M. Coumarin as a Quantitative Probe for Hydroxyl Radical Formation in Heterogeneous Photocatalysis. *J. Phys. Chem. C* **2019**, *123*, 6667–6674. [[CrossRef](#)]
52. Li, L.; Hao, C.; Zhai, R.; He, W.; Deng, C. Study on the mechanism of free radical scavenger TEMPO blocking in coal oxidation chain reaction. *Fuel* **2023**, *331 Pt 2*, 125853. [[CrossRef](#)]
53. Miyosh, N.; Tomit, G. Quenching of Singlet Oxygen by Sodium Azide in Reversed Micellar Systems. *Z. Fur. Naturforsch.–B J. Chem.* **1979**, *34*, 339–343. [[CrossRef](#)]
54. Miyoshia, N.; Uedaa, M.; Fukeb, K.; Tanimotoa, Y.; Itoha, M.; Tomitac, G. Lifetime of Singlet Oxygen and Quenching by NaN₃ in Mixed Solvents. *Z. Fur. Naturforsch.–B J. Chem.* **1982**, *37*, 649–652. [[CrossRef](#)]
55. Bancirova, M. Sodium azide as a specific quencher of singlet oxygen during chemiluminescent detection by luminol and Cypridina luciferin analogues. *Luminescence* **2011**, *26*, 685–688. [[CrossRef](#)] [[PubMed](#)]
56. Della Greca, M.; Pinto, G.; Pistillo, P.; Pollio, A.; Previtiera, L.; Temussia, F. Biotransformation of ethinylestradiol by microalgae. *Chemosphere* **2008**, *70*, 2047–2053. [[CrossRef](#)] [[PubMed](#)]
57. Maumy, M.; Capdevielle, P. Chemical Evidence for Peroxy Radicals Intermediacy in Copper(II) Reaction with Hydroperoxides. *Tetrahedron* **1993**, *49*, 1455–1462. [[CrossRef](#)]